Received: 16 December 2019 | Accepted: 21 January 2020 | Published online: 13 April 2020

DOI: 10.1002/dad2.12013

Alzheimer's & Dementia
Diagnosis, Assessment & Disease Monitoring

DIAGNOSTIC ASSESSMENT & PROGNOSIS

Down syndrome: Distribution of brain amyloid in mild cognitive impairment

David B. Keator[1] | Michael J. Phelan[2] | Lisa Taylor[1] | Eric Doran[3] | Sharon Krinsky-McHale[4] | Julie Price[5] | Erin E. Ballard[1] | William C. Kreisl[6] | Christy Hom[1] | Dana Nguyen[1] | Margaret Pulsifer[5] | Florence Lai[5] | Diana H. Rosas[5] | Adam M. Brickman[7] | Nicole Schupf[7] | Michael A. Yassa[1,8] | Wayne Silverman[3] | Ira T. Lott[3]

[1]Department of Psychiatry and Human Behavior, University of California, Irvine, California

[2]Institute for Memory Impairments and Neurological Disorders, UC, Irvine, California

[3]Department of Pediatrics, University of California, Irvine Medical Center, Orange, California

[4]New York State Institute for Basic Research in Developmental Disabilities, New York, New York

[5]Massachusetts General Hospital, Harvard University, Boston, Massachusetts

[6]Department of Neurology, Columbia University, New York, New York

[7]Department of Neurology and of Epidemiology, Columbia University, New York, New York

[8]Department of Neurobiology and Behavior and Center for the Neurobiology of Learning and Memory, University of California, Irvine, California

Correspondence
David B. Keator, University of California, Irvine, Irvine Hall rm. 163, ZOT-3961, Irvine, CA 92697.
Email: dbkeator@uci.edu

Funding information
National Institute on Aging, Grant/Award Number: U01AG051412-01; NICHD, Grant/Award Numbers: 065160, R01 AG053555, P50 AG16573

Abstract

Introduction: Down syndrome (DS) is associated with a higher risk of dementia. We hypothesize that amyloid beta (Aβ) in specific brain regions differentiates mild cognitive impairment in DS (MCI-DS) and test these hypotheses using cross-sectional and longitudinal data.

Methods: 18F-AV-45 (florbetapir) positron emission tomography (PET) data were collected to analyze amyloid burden in 58 participants clinically classified as cognitively stable (CS) or MCI-DS and 12 longitudinal CS participants.

Results: The study confirmed our hypotheses of increased amyloid in inferior parietal, lateral occipital, and superior frontal regions as the main effects differentiating MCI-DS from the CS groups. The largest annualized amyloid increases in longitudinal CS data were in the rostral middle frontal, superior frontal, superior/middle temporal, and posterior cingulate cortices.

Discussion: This study helps us to understand amyloid in the MCI-DS transitional state between cognitively stable aging and frank dementia in DS. The spatial distribution of Aβ may be a reliable indicator of MCI-DS in DS.

KEYWORDS

ABC-DS, ADDS, Alzheimer's disease, amyloid, AV-45, dementia, Down syndrome, MCI, PET

1 | INTRODUCTION

Studying adults with Down syndrome (DS) provides valuable insight into the nature and progression of Alzheimer's disease (AD). The predominant genetic basis of DS is a triplication of chromosome 21, which contains, among others, the amyloid precursor protein (APP). Of interest, individuals with DS may be at a higher risk for developing AD compared to other individuals with intellectual disability,[1,2] with the triplication and overexpression of APP playing a key role. This has been demonstrated by studies of rare partial trisomy cases in which there are two copies of APP and no resultant dementia or neuropathological findings for AD.[3,4] In DS, virtually all have amyloid beta (Aβ) plaques and tau-based neurofibrillary pathology consistent with a neuropathological determination of AD by age 40,[5] and after age 60 the prevalence of clinical AD is reported to be at 75% or higher.[6–8]

Several considerations justify advancing our understanding of AD progression in adults with DS. On one hand, birth incidence remains stable while life expectancy has increased, creating a significant patient population.[9,10] On the other hand, adults with DS represent the largest population at genetically high risk for AD, making them an attractive focus for research in understanding AD progression. This second consideration is strengthened by the fact that risk for other progressive neuropathologies in DS is relatively low.[11] Thus, older adults with DS represent an important population for studying AD progression.

Interventions targeting Aβ plaques after the clinical onset of dementia have been predominantly unsuccessful,[12] suggesting a need for early biomarkers predictive of conversion. Positron emission tomography (PET) has been used to measure Aβ in the brain through the development of tracers that are sensitive to Aβ plaques.[13,14] Specifically, the ^{18}F-AV-45 (florbetapir) ligand detects fibrillar Aβ concentration in people with DS[15] and sporadic AD.[16] Recent PET studies highlight the importance of a regional analysis of brain Aβ in participants with DS.[17] First, using ^{18}F-AV-45, Sabbagh et al.[18] reported differential patterns of amyloid in the inferior parietal, superior temporal, and prefrontal cortex in DS based on differences between a sample of 5 participants clinically diagnosed with AD and 12 without (average age 50 and 36 years, respectively). Second, Annus et al. studied younger adults[19] using [^{11}C] Pittsburgh Imaging Compound B (PiB) to evaluate Aβ load in DS. Their results showed that binding first appeared in the striatum at around 40 years of age, and PiB positivity correlated with the number of distinct regions having amyloid above an empirically defined threshold for positivity, consistent with other groups.[17,20] Third, in a longitudinal PET study, Lao et al.[21] reported differential mean annualized percent changes in amyloid load as a function of brain region and PiB positivity status. Finally, in a pilot study using ^{18}F-AV-45, we showed that the timing of conversion to dementia in five transitioned participants with DS was associated with s higher load in sub-regions of frontal, temporal, parietal, and cingulate cortices.[22]

Taken together, these studies suggest that characterization of the spatial distribution and region-specificity of Aβ will likely inform our understanding of dementia pathogenesis in DS. The results of our previous work,[22] in particular, support the proposal that increases in specific brain regions may be strongly associated with at least the early stages of conversion to AD.

The current study was designed to validate these previous findings in a large independent sample and a longitudinal cohort of adults with DS. In this context, we focus on individuals with DS and mild cognitive impairment (MCI-DS). MCI-DS is considered an early stage of clinical progression of AD preceding a diagnosis of dementia, and offers the possibility of identifying an early stage of amyloid deposition. The first aim of this study was to test whether amyloid load in a priori selected regions is higher in participants with MCI-DS compared to cognitively stable (CS) individuals. The second aim was to estimate the within-subject amyloid changes in a longitudinal cohort of CS participants with the expectation of showing consistent patterns of differential increases.

RESEARCH IN CONTEXT

1. Systematic review: The authors reviewed the Down syndrome (DS) literature through typical methods using PubMed, reviews of conference publications, abstracts, and posters. Prior publications are focused on empirically defined groups based on amyloid load and cited in our article. The current study characterizes brain amyloid distributions in mild cognitive impairment in DS (MCI-DS). This study is the first to characterize brain amyloid distributions in MCI-DS using a large cohort.
2. Interpretation: The study confirmed our hypotheses of increased amyloid in inferior parietal, lateral occipital, and superior frontal regions as the main effect differentiating MCI-DS from cognitively stable (CS) individuals. The largest annualized amyloid increases in longitudinal CS data were in rostral middle frontal, superior frontal, superior/middle temporal, and posterior cingulate cortices.
3. Future directions: Our future work will expand our sample and follow participants longitudinally to understand amyloid and tau signatures in MCI-DS and the identification of composite biomarkers that predict clinical transition.

2 | METHODS

2.1 | Participant characteristics

This study included a subset of participants from the Alzheimer's Biomarkers Consortium–Down Syndrome (ABC-DS),[23] a multisite, multidisciplinary program to identify biomarkers associated with AD in adults with DS. Research procedures were reviewed and approved by the institutional review boards, and informed consent/assent was

obtained from all participants and their legal representatives. The researchers and authors of this paper have no competing interests to declare. Here we report on 85 participants (40-64 years of age) imaged with ^{18}F-AV-45 PET and who have completed the first of three longitudinal cycles at the following sites: Massachusetts General Hospital/Harvard University (MGH), Columbia University, the New York State Institute for Basic Research in Developmental Disabilities and University of California, Irvine (UCI). Twelve participants had a previous imaging session acquired 3.8 ± 0.97 years prior to their current evaluation and reported in Keator et al.[22] All remained cognitively stable over this time. Of the 85 participants, 6 were not included in the analysis due to artifacts identified in the scans. Omission of these cases was confirmed by a local outlier factor (LOF) analysis computed across a range of neighborhood settings ($\{k \in \mathbb{N} | 5 \leq k \leq 15\}$), where an a priori–defined LOF score >2.0 in any neighborhood was identified as an outlier.[24]

2.2 | Determination of dementia status using consensus conference procedures

Each participant's clinical status was evaluated with a standardized assessment battery including detailed review of medical records, informant interviews regarding functional/vocational abilities and neuropsychiatric concerns, direct assessment of a variety of cognitive abilities, maladaptive behaviors and neuropsychiatric symptoms, and health status. The diagnostic status of each participant was rated at a consensus case conference using data from all sources but was blind to any imaging or fluid biomarker findings.[25–27]

Clinical status was classified into the following categories: (1) cognitively stable (or CS), indicating with reasonable certainty that clinically significant declines beyond those of normal aging were absent; (2) MCI-DS, indicating there was some mild cognitive/functional decline greater than would be expected with aging but not sufficiently severe to meet criteria for dementia, (3) possible dementia (DEM), indicating that some signs/symptoms of dementia were present, but declines over time were not totally convincing; (4) definite dementia (or DEM), indicating a high degree of confidence that dementia was present; or (5) status uncertain, indicating that the evidence of decline was present but one or more factors unrelated to an aging-associated neuropathology might be the cause.

In this study we focus on characterizing cross-sectional regional brain amyloid in participants with MCI-DS and longitudinally in participants before MCI-DS onset. Although the possible + probable dementia (DEM) group is more affected cognitively, we were uncomfortable drawing any conclusions due to the small sample size, but have included information in the supplement and highlighted differences from MCI-DS in the discussion. We anticipate formal analysis of the DEM group when the sample size warrants. Among the cross-sectional data, the CS group differed in mean age from the MCI-DS ($t[33.68] = -3.70$; $P < .001$ two-tailed) and DEM groups ($t[10.34] = -3.74$; $P < .004$ two-tailed), as did sex ($P < .056$ Fisher exact test).

2.3 | Image acquisition

^{18}F-AV-45 PET scans were acquired for each participant at their enrollment site. Participants at UCI were scanned on a High Resolution Research Tomograph (HRRT; orientation = axial, voxel size = 1.2 mm^3, matrix size = 256 × 256 × 207, reconstruction = Ordinary Poisson Ordered Subset Expectation Maximation (OP-OSEM)), at Columbia on a Siemens Biograph64 mCT (orientation = axial, voxel size = 1.0 × 1.0 × 2.0 mm, matrix size = 400 × 400 × 436, reconstruction = OSEM3D+Time Of Flight (TOF) 4i21s), and MGH on a Siemens Biograph mMR (orientation = axial, voxel size = 2.1 × 2.1 × 2.0 mm, matrix size = 344 × 344 × 127, reconstruction = OP-OSEM 3i21s). Image acquisition followed the Alzheimer's Disease Neuroimaging Initiative (ADNI)[28,29] protocol: 4 × 5 minute frames collected 50 to 70 minutes after injection. PET reconstructions were performed with attenuation and scatter correction as implemented on each platform. T1-weighted magnetic resonance imaging (MRI) scans were acquired using ADNI protocols. Participants at UCI were scanned on a Philips Achieva 3T (orientation = sagittal, repetition time/echo time [TR/TE] = 7.8/3.6 ms, flip angle = 7°, voxel size = 1 mm^3, matrix size = 256 × 256 × 176) or a Siemens Prisma 3T (orientation = sagittal, inversion time[TI]/TR/TE = 900/2300/3.0 ms, flip angle = 9°, voxel size = 1 mm^3, matrix size = 240 × 256 × 208). Both Columbia and MGH used a Siemens Prisma 3T scanner.

2.4 | Image processing

The reconstructed PET frames were realigned and averaged prior to analysis and then co-registered with their respective MRI studies. For region of interest (ROI) analyses and standardized uptake value ratio (SUVR) scaling, MRI segmentations were computed with FreeSurfer (FS6 version 6.0; RRID:SCR_001847),[30–32] visually checked for accuracy, and corrected when necessary using procedures from FreeSurfer. PET counts were converted to SUVR units using the cerebellum-cortex reference region prior to computing ROI averages. MRI-derived voxel-weighted SUVR averages for each ROI were extracted in native space using the Desikan/Killiany atlas.[33] For voxel-based analyses, images were aligned to the Montreal Neurological Institute (MNI) space with Advanced Normalization Tools (ANTs version 2.2.0;[34] RRID:SCR_004757), aligning the MRI scans to a DS average target in MNI space and applying the transformations to the co-registered PET scans. Voxel-based image analysis was performed with the SPM12 Statistical Parametric Mapping tool (RRID:SCR_007037).

To account for the differences in spatial resolution of the PET acquisition platforms, data from UCI's HRRT were smoothed to the reconstructed spatial resolutions of the Biograph mMR and Biograph64. The resulting images were inspected visually for similarity across sites. The ROI and voxel-based results using this "smoothed-to" data are reported in this article. We further evaluated the consistency of our results using partial volume corrected (PVC) data with PETSurfer,[35,36] correcting for the platform-specific published spatial resolution of each imaging system. In addition to the above correction methods, acquisition site was

TABLE 1 Participant characteristics showing total N within each diagnosis, sex, *APOE* status, and mean (±SD) age at time of PET scan

Diagnosis	N	Sex	*APOE* Status e4/no e4/unknown	Age PET 1 (years) [min, max]	Age PET 2 (years) [min, max]
Cognitively stable (CS)	41	18F/23 M	9/29/3	46 ± 5.6 [40, 59]	
Mild cognitive impairment (MCI-DS)	17	2F/15 M	8/8/1	52 ± 5.0 [44, 62]	
Dementia (DEM)	9	4F/5 M	4/5/0	56 ± 7.0 [45, 65]	
Longitudinal CS	12	2F/10 M	1/11/0	50 ± 4.0 [43, 57]	54 ± 4.6 [46, 62]

added as a covariate to account for additional sources of site-related variance.

2.5 | Data analysis

Here we report on analyses about specific brain regions (sub-regions of frontal, temporal, parietal, occipital, and cingulate cortices) for which amyloid load is expected to increase from CS to MCI-DS. Along with our expected regions, we have included two composite regions: (1) from Jack et al.[37] for defining imaging biomarker cut points in AD (Jack2017Composite), consisting of the voxel-weighted average of prefrontal, orbitofrontal, parietal, temporal, anterior and posterior cingulate, and precuneus regions; and (2) from Keator et al.[22] consisting of the voxel-weighted average of inferior parietal, superior temporal, frontal, and anterior cingulate (Keator2018Composite). In addition, we included two "control" regions: hippocampus and entorhinal cortex (EC). We observed no relationship between amyloid and transition in Keator et al.[22] in these two regions and therefore did not expect to observe increased amyloid in MCI-DS compared to the CS group, or in the longitudinal CS cohort. Finally, we included the dorsal striatum, a region of early amyloid binding in DS and therefore expected it to be informative in characterizing amyloid in MCI-DS.[38,39]

TABLE 2 Estimates of successive percentage difference in SUVR for CS versus MCI-DS

Region	Estimate (lower, upper)	SE	*P* unc.	Adj. *P*
Inferior parietal*	10.70 (0.69, 21.69)	4.83	.018	.162
Lateral occipital*	10.65 (0.11, 22.30)	5.12	.024	.187
Superior frontal*	10.54 (−0.39, 22.66)	5.32	.029	.206
Keator2018Composite*	8.41 (−0.74, 18.40)	4.49	.036	.215
Jack2017Composite*	8.25 (−0.65, 17.94)	4.37	.035	.209
Rostral middle frontal	8.28 (−2.68, 20.48)	5.46	.070	.239
Inferior temporal	7.93 (−2.65, 19.66)	5.28	.072	.239
Anterior cingulate	7.33 (−1.86, 17.38)	4.56	.059	.238
Superior temporal	7.00 (−1.91, 16.70)	4.42	.062	.239
Dorsal striatum	6.50 (−2.12, 15.88)	4.30	.070	.239
Middle temporal	6.07 (−2.90, 15.87)	4.50	.093	.269
Posterior cingulate	5.93 (−2.57, 15.18)	4.26	.086	.259
Medial orbitofrontal	4.98 (−4.81, 15.76)	4.99	.162	.324
Orbitofrontal	4.46 (−4.13, 13.82)	4.37	.156	.312
Hippocampus	4.34 (−1.62, 10.66)	2.98	.077	.239
Lateral orbitofrontal	3.85 (−4.30, 12.69)	4.16	.179	.358
Entorhinal cortex	−0.14 (−5.40, 5.41)	2.73	.521	.521

Comparisons are grouped within ROI. Estimates are in percent difference adjusted for key covariates along with 95% lower, upper confidence intervals on 52 degrees of freedom (dof). *P*-values (uncorrected and adjusted) are one-sided for hypothesized positive differences.

3 | RESULTS

3.1 | Cross-sectional analyses

For cross-sectional ROI analyses comparing MCI-DS to CS, linear models (RStudio version 1.1.447; RRID:SCR_001905[40]) were fit regressing each ^{18}F-AV-45 ROI average (treated separately) on additive indicators of diagnosis, sex, and site. Age and ROI volume were included as quantitative covariates. Mean difference estimates were extracted from the group coefficient and 95% confidence intervals (CIs) were calculated and reported for the population values. For voxel-based analyses, a multiple regression model was fit (SPM12) which included analysis of covariance (ANCOVA) global normalization, age, sex, site, and diagnosis.

Estimates of successive adjusted percent differences in the "smoothed-to" mean SUVR values for both MCI-DS and CS groups along with the standard errors (SEs), 95% CIs, and one-sided uncorrected and adjusted *P*-values for our hypothesized positive changes in amyloid are shown in Table 2. *P*-values were adjusted using a Bonferroni-Hommel method.[41] The largest percent differences between MCI-DS and CS were in the inferior parietal, lateral occipital, and superior frontal regions (≈10%), followed by the Keator2018Composite, rostral middle frontal, and Jack2017Composite regions (≈8%). The smallest differences were in the temporal regions, orbitofrontal cortices, dorsal striatum, and the cingulate regions (≈4%-7%). These effects were consistent using the PVC-corrected data, yet the estimated mean differences were much higher in the inferior parietal and superior frontal regions (≈24%), superior temporal and rostral middle frontal regions (≈11% and 13%), and the dorsal striatum (11%). None of the regions survived the Hommel multiple comparison procedure at the $P < .05$ (shown in Figure 1), but this was not surprising given the conservative nature of this correction and the limited statistical power inherent in the sample sizes.

Forest plots are provided in Figure 1 for unadjusted (left) and adjusted data (right) after removing linear associations with age,

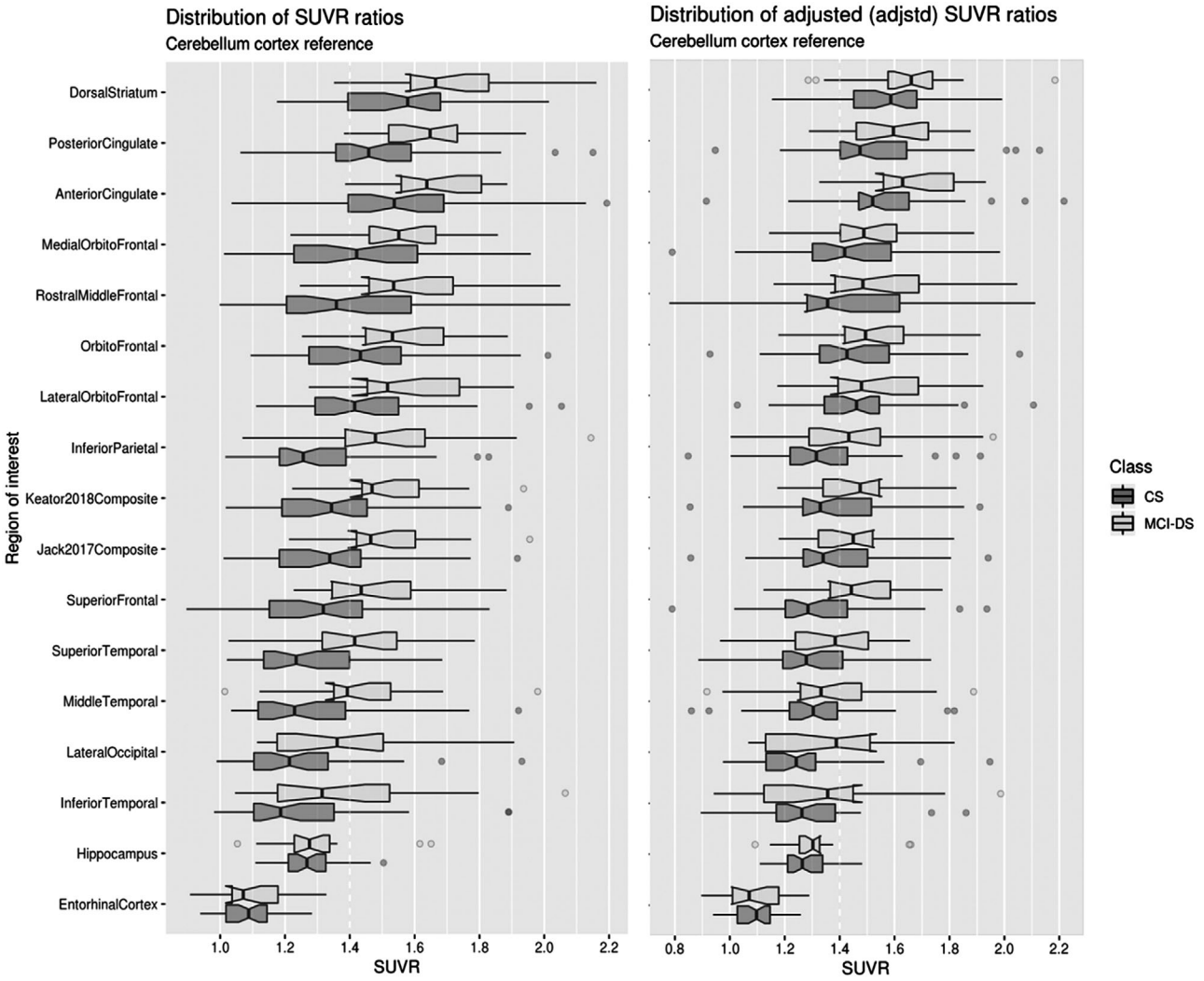

FIGURE 1 Plots showing distributions of unadjusted marginal estimates for each region by diagnosis (left) and the adjusted data (right) after removing the linear associations with age, sex, acquisition site, and region of interest (ROI) volume, scaled to the mean/standard deviation of the CS group

volume, site, and sex. Residuals were centered and scaled to the overall CS mean and standard deviation (SD). Regions were ordered by the MCI-DS unadjusted median SUVR value. The vertical line at 1.4 SUVR may be suggestive of amyloid positivity in the non-DS population[37] and is included as a reference value. Although the largest differences between the groups were in the inferior parietal, lateral occipital, and superior frontal regions, the highest SUVR average was in the dorsal striatum, a region identified as having the earliest amyloid in DS,[38,39] followed by the posterior/anterior cingulate, another region shown to have increased PiB retention in DS.[42]

To further understand group differences in regional distribution, a voxel-based linear regression was performed in SPM12 using ANCOVA scaling and indicators of diagnosis, sex, site, and scan age. T-maps were then converted to estimated effect-size maps (Figure 2) using the f-modeling approach to empirical Bayes estimation.[43] Regions with large effect sizes are key to understanding the role of amyloid accumulation in disease progression. Generally, the voxel-based analyses were consistent with the ROI results, with large effect sizes (>2.0) in the superior frontal, rostral middle frontal, inferior parietal, and lateral occipital regions ($P < .001$ uncorrected (unc)). Unlike the ROI data, there were equally large effect sizes (>2.0) in the superior, middle, and inferior temporal regions ($P < .001$unc). The anterior and posterior cingulate had moderate effect sizes ranging from 1.5 to 2.0. The dorsal striatum effect size was unremarkable. The voxel-based analysis provided information beyond our a priori hypothesized regions for which we see effect sizes in the thalamus, superior parietal, postcentral, precentral, fusiform, caudal-middle-frontal, pars-opercularis, pars-triangularis, and cuneus/precuneus ranging from 1.5 to 3.2.

3.1.1 | Longitudinal analysis

In the cross-sectional analysis we observed evidence supporting our hypotheses of increased amyloid load in the superior frontal, inferior

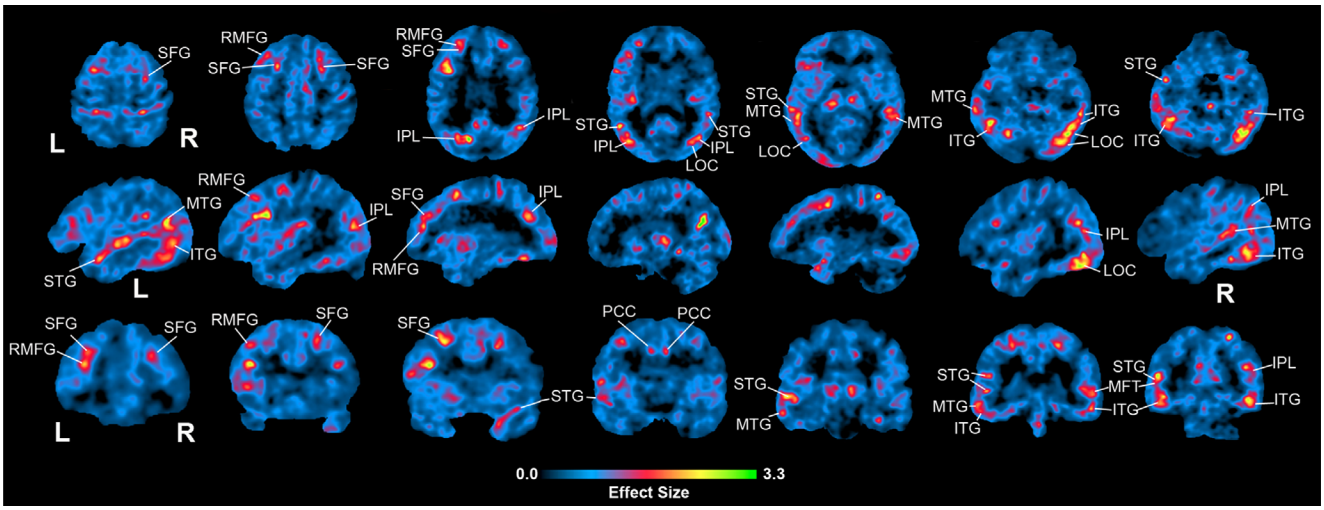

FIGURE 2 Voxel-based contrasts of the MCI-DS versus CS groups showing effect sizes of increased amyloid load in MCI-DS compared to CS. Areas of increase corresponding to a priori hypothesized regions are labeled with abbreviations: IPL = inferior parietal lobe; ITG = inferior temporal gyrus; LOC = lateral occipital cortex; LOF = lateral orbitofrontal; MTG = middle temporal gyrus; RMFG = rostral middle frontal gyrus; PCC = posterior cingulate cortex; SFG = superior frontal gyrus; STG = superior temporal gyrus

parietal, and lateral occipital regions as the strongest indicators of MCI-DS development. We now return to the original cohort of 12 unaffected participants from our previous study,[22] who were scanned a second time ≈4 years later (3.8 ± 0.97 years) and remained cognitively stable. We predicted that cognitively stable older participants would show evidence of increasing amyloid load in regions most strongly indicative of MCI-DS as they age and theoretically approach clinical transition. We acknowledge this is not a completely independent sample, since the first scan was used in the transition study[22] and contributed to our a priori identified regions for this study. However, evaluating the change in these participants, who have not yet transitioned to MCI-DS, provides additional empirical support for our regional hypotheses and transition into clinically evident disease states.

In Figure 3 we show the SUVRs of the latest (T1) to the earliest amyloid scan (T0), ordered by magnitude of increase. Data points are colored according to the temporal interval (T1-T0). Similar to the cross-sectional analyses, we see the largest increases in the frontal and parietal lobes, followed by the posterior cingulate, dorsal striatum, and middle temporal lobe. Both composite ROIs are also sensitive to these increases. Note the large variability in the ratios across participants, which is not surprising given the continuous nature of the disease process and individual differences in the rate of progression within that spectrum. Table 3 shows the annualized percent change in SUVR, ordered by magnitude of the mean change. The ordering is similar to the longitudinal ratios except in the superior temporal lobe showing a higher relative percent change. Of interest, the superior temporal lobe was among the most significant regions differentiating transitioned from non-transitioned participants after sub-regions of the frontal lobe in our previous study,[22] and may be accumulating amyloid earlier than the frontal regions as AD progresses preclinically, and then reaching a plateau. This would result in a lower overall ranking as compared to some of the other regions when comparing CS to MCI-DS. As expected, the control regions (ie, EC and hippocampus) showed nominal changes.

TABLE 3 Estimates of the average percentage change in SUVR per year along with 95% lower, upper confidence intervals, adjusted for the years between scans, and DOF = 11

ROI	%-change (lower, upper)	SE	*P* unc.	*P* adj.
Rostral middle frontal	4.1 (1.5, 6.8)	1.2	.005	.025
Superior frontal	4.1 (1.6, 6.7)	1.1	.004	.020
Keator2018Composite	3.4 (1.4, 5.4)	0.9	.003	.018
Jack2017Composite	3.2 (1.4, 5.1)	0.8	.002	.016
Superior temporal	3.2 (1.4, 5.0)	0.8	.002	.016
Posterior cingulate	3.1 (1.2, 5.0)	0.9	.005	.025
Middle temporal	3.0 (1.5, 4.6)	0.7	.001	.012
Dorsal striatum	2.9 (0.9, 5.0)	0.9	.009	.036
Anterior cingulate	2.8 (0.9, 4.7)	0.8	.007	.028
Inferior parietal	2.6 (1.0, 4.2)	0.7	.004	.020
Inferior temporal	2.5 (1.1, 3.9)	0.6	.002	.016
Medial orbitofrontal	2.4 (1.0, 3.9)	0.7	.004	.020
Orbitofrontal	2.4 (0.8, 4.0)	0.7	.006	.025
Lateral orbitofrontal	2.4 (0.7, 4.1)	0.8	.010	.040
Entorhinal cortex	1.2 (0.0, 2.4)	0.6	.052	.156
Lateral occipital	0.9 (−0.6, 2.5)	0.7	.205	.410
Hippocampus	0.1 (−1.3, 1.6)	0.7	.870	.870

ROIs are ordered in decreasing order of the magnitude of the mean change. *P*-values (uncorrected and adjusted) are one-sided for hypothesized positive differences.

4 | DISCUSSION

In this study, we presented both cross-sectional and longitudinal analyses of amyloid in prodromal and preclinical stages of AD. In our prior work,[22] we identified sub-regions of frontal, temporal, parietal, occipital, and cingulate cortices that were associated with increased

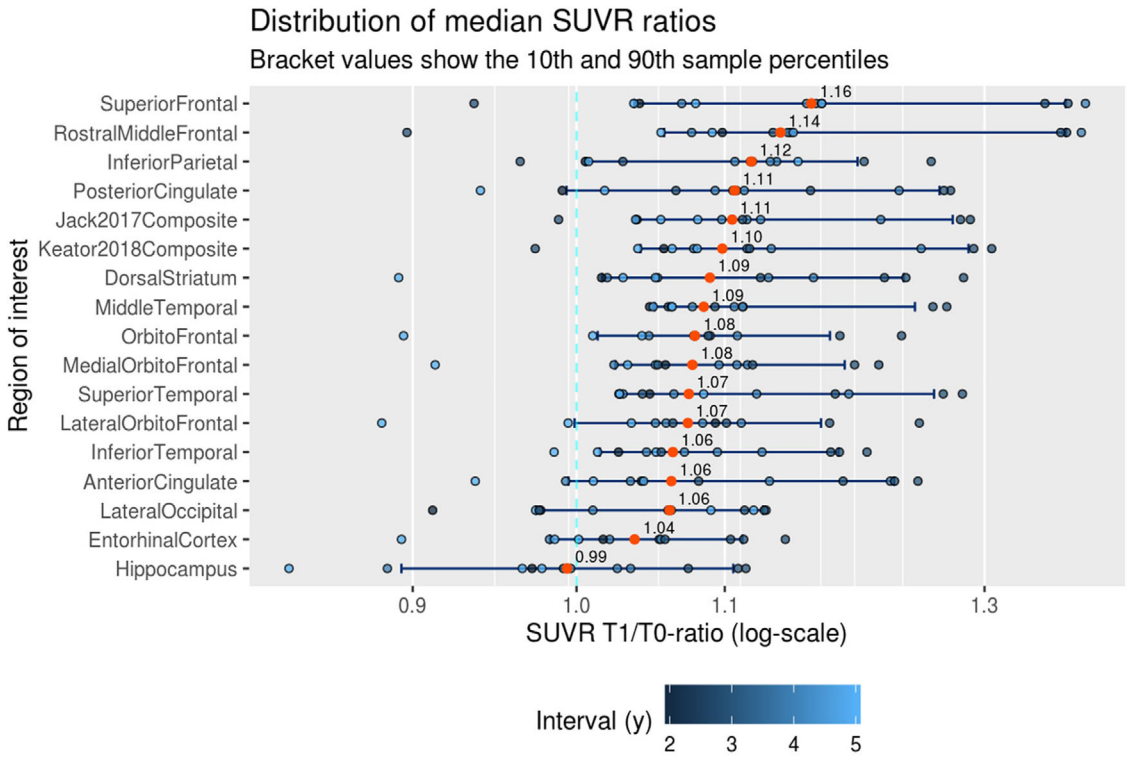

FIGURE 3 Distribution of standardized uptake value ratios (SUVRs) (T1/T0) by region of interest (ROI). Regions are ordered, smallest to largest, with respect to the median ratio. Bracket values mark the 10th and 90th percentiles of the sample, giving a near complete representation of the distribution of values. Values are plotted with a color scale based on the interval between scans. Red circles represent the median value

amyloid and dementia status. Here we found supporting evidence for our hypotheses using an independent cross-sectional cohort and longitudinal data. Our results generally agreed with our prior study associating increased amyloid in specific regions with early cognitive impairment in DS.

Beyond validating our hypotheses, this study helped us understand how amyloid load differs in the MCI-DS transitional state between cognitively stable aging and frank dementia. Consistent with prior work, we see high dorsal striatum amyloid load in the MCI-DS group. This region was identified previously in younger participants with DS and is often used to separate participants into amyloid positive/negative groups.[38,39] In our data, the dorsal striatum has the highest median SUVR value of the regions evaluated. However, it was not among the best regions for separating MCI-DS from CS groups, and even less so in our small DEM group (Supplementary sections 1, 2). This may be evidence of a plateau temporally near the transition to clinical progression, although lack of sufficient statistical power is also possible.

A result that differed from our prior study[22] is the weaker relationship between orbital-frontal amyloid and diagnosis. Previously, we found that medial/lateral orbital-frontal amyloid was a strong predictor of transition. Of interest, in the DEM cohort (n = 9), we observed increased amyloid in orbital-frontal regions when contrasting DEM versus CS and DEM versus MCI-DS groups (Supplementary sections 1, 2). Furthermore, we see a clear orbito-frontal pattern of large effect sizes in the DEM group. These results suggest that our MCI-DS group is likely at an earlier stage of cognitive decline compared to the participants that transitioned in our prior study, and increases in orbital-frontal amyloid are indicators of more advanced disease progression in DS.

Looking more broadly at our voxel-based analyses, we see large effect sizes in the thalamus. The thalamus was not a region identified in our prior work as predictive of transition. Specifically, the cluster on the right is located in the medial dorsal nucleus (MNI: 7.9, −18.1, 4.0 mm), which is structurally connected to the prefrontal cortex.[44–46] The cluster on the left is located in the ventral nuclear group (MNI: −14.4, −22.3, 4.0 mm) and is structurally connected to the posterior parietal, sensory, and primary motor cortices.[44–46] Although there have not been associations between amyloid propagation and structural connectivity reported, there is evidence of associations with tau pathology.[47] We plan to investigate whether structural tract changes predict tau pathology in the presence of amyloid[48] with future tau PET scans.

With respect to our control regions, EC and hippocampus, we observed small longitudinal changes in EC and almost no change in the hippocampus. No effects approached statistical significance and we therefore concluded that no substantial evidence of amyloid differences in either of these regions associated with preclinical or prodromal AD progression within our DS sample.

Although our study is a relatively large sample of DS participants, it is still underpowered. Furthermore, differentiating MCI and early dementia in DS objectively is complicated by variation in severity and specific profiles of preexisting cognitive impairment.[26] Due to our small

sample of female participants diagnosed with MCI-DS, we were also unable to evaluate relevant sex differences.

Notwithstanding these limitations, our study used state-of-the-art procedures for diagnostic classification in populations with intellectual disabilities, which we believe provides accuracy in diagnoses, approaching that for neurotypical populations. We based our analyses on a priori–identified regions, evaluated our hypotheses in an independent cross-sectional cohort, and further strengthened using a longitudinal cohort. Previous studies have suggested that there is so much amyloid uptake in DS from a young age that amyloid PET may not be of use in tracking the progress of AD. However, based on the consistency of our results, we feel confident that the unique brain amyloid signatures discussed here are reliable indicators of AD progression in DS. Our future work will consist of expanding and following our current sample longitudinally. We expect that the rich longitudinal data set will help us further confirm our inferences, provide us with the opportunity to evaluate amyloid and tau signatures in MCI-DS, and evaluate the identification of composite biomarkers that predict transitions from cognitively stable to mild cognitive impairment and eventual dementia.

ACKNOWLEDGMENTS

The preparation of this manuscript was made possible from data obtained by the Alzheimer's Disease in Down Syndrome (ADDS) component of the Alzheimer's Biomarkers Consortium–Down Syndrome (ABC-DS), a longitudinal study of Alzheimer Disease biomarkers in adults with Down syndrome, which is supported by grants from the National Institute on Aging (NIA) (U01AG051412-01 Schupf, Lott, Silverman) and the Eunice Kennedy Shriver National Institute of Child Health and Human Development (NICHD). Baseline longitudinal data were supported by previous grants from the NICHD (065160 (Lott), R01 AG053555 (May), and P50 AG16573 (May)). The primary goal of ABC-DS is to understand the factors that moderate the relationship between Aβ, neurodegeneration, and dementia in DS and biomarkers for those factors that could be critically important in the design of effective therapeutic trials for AD, not only in DS, but in the general population as well.

CONFLICTS OF INTEREST

The Co-Principal Investigators of the ADDS component of the ABC-DS program are Nicole Schupf, PhD, Doctor of Public Health (DrPh) (Columbia University), Ira Lott, MD, and Wayne Silverman, PhD (UC Irvine). Co-Principal Investigators of the NiAD ABC-DS component are Benjamin Handen, PhD and William Klunk, MD, PhD (University of Pittsburgh), and Bradley Christian, PhD (University of Wisconsin-Madison)

REFERENCES

1. Heller T, Scott HM, Janicki MP, Pre-Summit Workgroup on Caregiving and Intellectual/Developmental Disabilities. Caregiving, intellectual disability, and dementia: report of the Summit Workgroup on Caregiving and Intellectual and Developmental Disabilities. *Alzheimers Dement*. 2018;4:272-282.
2. Strydom A, Shooshtari S, Lee L, et al. Dementia in older adults with intellectual disabilities-epidemiology, presentation, and diagnosis. *J Policy Pract Intellect Disabil*. 2010;7:96-110.
3. Prasher VP, Farrer MJ, Kessling AM, et al. Molecular mapping of Alzheimer-type dementia in Down's syndrome. *Ann Neurol*. 1998;43:380-383.
4. Doran E, Keator D, Head E, et al. Down syndrome, partial trisomy 21, and absence of Alzheimer's disease: the role of APP. *J Alzheimers Dis*. 2017;56:459-470.
5. Head E, Lott IT, Wilcock DM, Lemere CA. Aging in down syndrome and the development of Alzheimer's disease neuropathology. *Curr Alzheimer Res*. 2015;13:18-29.
6. Zigman WB, Lott IT. Alzheimer's disease in Down syndrome: neurobiology and risk. *Ment Retard Dev Disabil Res Rev*. 2007;13:237-246.
7. Lai F, Williams RS. A prospective study of Alzheimer disease in Down syndrome. *Arch Neurol*. 1989;46:849-853.
8. Evenhuis HM. The natural history of dementia in Down's syndrome. *Arch Neurol*. 1990;47:263-267.
9. Silverman W. Down syndrome: cognitive phenotype. *Ment Retard Dev Disabil Res Rev*. 2007;13:228-236.
10. Rasmussen SA, Whitehead N, Collier SA, Frías JL. Setting a public health research agenda for Down syndrome: summary of a meeting sponsored by the Centers for Disease Control and Prevention and the National Down Syndrome Society. *Am J Med Genet A*. 2008;146A:2998-3010.
11. Bayen E, Possin KL, Chen Y, Cleret de Langavant L, Yaffe K. Prevalence of aging, dementia, and multimorbidity in older adults with Down syndrome. *JAMA Neurol*. 2018;75:1399-1406.
12. Anderson RM, Hadjichrysanthou C, Evans S, Wong MM. Why do so many clinical trials of therapies for Alzheimer's disease fail?. *Lancet*. 2017;390:2327-2329.
13. Klunk WE, Engler H, Nordberg A, et al. Imaging brain amyloid in Alzheimer's disease with Pittsburgh Compound-B. *Ann Neurol*. 2004;55:306-319.
14. Wong DF, Rosenberg PB, Zhou Y, et al. In vivo imaging of amyloid deposition in Alzheimer disease using the radioligand 18F-AV-45 (flobetapir F 18). *Eur J Nucl Med*. 2010;51:913-920.
15. Sabbagh MN. Positron emission tomography and neuropathologic estimates of fibrillar amyloid-β in a patient with Down syndrome and Alzheimer disease. *Arch Neurol*. 2011;68:1461.
16. Camus V, Payoux P, Barré L, et al. Using PET with 18F-AV-45 (florbetapir) to quantify brain amyloid load in a clinical environment. *Eur J Nucl Med Mol Imaging*. 2012;39:621-6231.
17. Handen BL, Cohen AD, Channamalappa U, et al. Imaging brain amyloid in nondemented young adults with Down syndrome using Pittsburgh compound B. *Alzheimers Dement*. 2012;8:496-501.
18. Sabbagh MN, Chen K, Rogers J, et al. Florbetapir PET, FDG PET, and MRI in Down syndrome individuals with and without Alzheimer's dementia. *Alzheimers Dement*. 2015;11:994-1004.
19. Annus T, Wilson LR, Hong YT, et al. The pattern of amyloid accumulation in the brains of adults with Down syndrome. *Alzheimers Dement*. 2016;12:538-545.
20. Hartley SL, Handen BL, Devenny DA, et al. Cognitive functioning in relation to brain amyloid-β in healthy adults with Down syndrome. *Brain*. 2014;137:2556-2563.
21. Lao PJ, Handen BL, Betthauser TJ, et al. Longitudinal changes in amyloid positron emission tomography and volumetric magnetic resonance imaging in the nondemented Down syndrome population. *Alzheimers Dement*. 2017;9:1-9.
22. Keator DB, Doran E, Van Erp TGM, et al. [18F]-Florbetapir PET: towards predicting dementia in adults with Down syndrome. *bioRxiv*. 2018:235440. https://doi.org/10.1101/235440.

23. Alzheimer's Biomarkers Consortium — Down Syndrome (ABC-DS). National Institute on Aging n.d. https://www.nia.nih.gov/research/abc-ds (accessed August 13, 2019).
24. Breunig MM, Kriegel H-P, Ng RT, Sander J. *LOF: Identifying Density-Based Local Outliers. Proceedings of the 2000 ACM SIGMOD International Conference on Management of Data - SIGMOD '00*. New York, New York, USA: ACM Press; 2000:93-104.
25. Silverman W, Schupf N, Zigman W, et al. Dementia in adults with mental retardation: assessment at a single point in time. *Am J Ment Retard*. 2004;109:111.
26. Silverman WP, Zigman WB, Krinsky-McHale SJ, Ryan R, Schupf N. Intellectual disability, mild cognitive impairment, and risk for dementia. *J Policy Pract Intellect Disabil*. 2013;10. https://doi.org/10.1111/jppi.12042.
27. Krinsky-McHale SJ, Silverman W. Dementia and mild cognitive impairment in adults with intellectual disability: issues of diagnosis. *Dev Disabil Res Rev*. 2013;18:31-42.
28. Landau SM, Breault C, Joshi AD, et al. Amyloid-imaging with Pittsburgh compound B and florbetapir: comparing radiotracers and quantification methods. *J Nucl Med*. 2012;54:70-77.
29. ADNI Home n.d. http://www.adni-info.org/ (accessed December 8, 2016).
30. FreeSurfer n.d. https://surfer.nmr.mgh.harvard.edu/ (accessed December 8, 2016).
31. Fischl B, Salat DH, Busa E, et al. Whole brain segmentation: automated labeling of neuroanatomical structures in the human brain. *Neuron*. 2002;33:341-355.
32. Fischl B, van der Kouwe A, Destrieux C, et al. Automatically parcellating the human cerebral cortex. *Cereb Cortex*. 2004;14:11-22.
33. Desikan RS, Ségonne F, Fischl B, et al. An automated labeling system for subdividing the human cerebral cortex on MRI scans into gyral based regions of interest. *Neuroimage*. 2006;31:968-980.
34. Avants BB, Tustison NJ, Song G, Cook PA, Klein A, Gee JC. A reproducible evaluation of ANTs similarity metric performance in brain image registration. *Neuroimage*. 2011;54:2033-2044.
35. Greve DN, Salat DH, Bowen SL, et al. Different partial volume correction methods lead to different conclusions: an (18)F-FDG-PET study of aging. *Neuroimage*. 2016;132:334-343.
36. Greve DN, Svarer C, Fisher PM, et al. Cortical surface-based analysis reduces bias and variance in kinetic modeling of brain PET data. *Neuroimage*. 2014;92:225-236.
37. Jack CR, Jr, Wiste HJ, Weigand SD, et al. Defining imaging biomarker cut points for brain aging and Alzheimer's disease. *Alzheimers Dement*. 2017;13:205-216.
38. Klunk WE, Price JC, Mathis CA, et al. Amyloid deposition begins in the striatum of presenilin-1 mutation carriers from two unrelated pedigrees. *J Neurosci*. 2007;27:6174-6184.
39. Cohen AD, McDade E, Christian B, et al. Early striatal amyloid deposition distinguishes Down syndrome and autosomal dominant Alzheimer's disease from late-onset amyloid deposition. *Alzheimers Dement*. 2018;14:743-750.
40. R: The R Project for Statistical Computing n.d. https://www.r-project.org (accessed August 14, 2019).
41. Hommel G. A stagewise rejective multiple test procedure based on a modified bonferroni test. *Biometrika*. 1988;75:383.
42. Hartley SL, Handen BL, Devenny D, et al. Cognitive decline and brain amyloid-β accumulation across 3 years in adults with Down syndrome. *Neurobiol Aging*. 2017;58:68-76.
43. Efron B. *Large-Scale Inference: Empirical Bayes Methods for Estimation, Testing, and Prediction*. Cambridge University Press; 2012.
44. Johansen-Berg H, Behrens TEJ, Sillery E, et al. Functional-anatomical validation and individual variation of diffusion tractography-based segmentation of the human thalamus. *Cereb Cortex*. 2005;15:31-39.
45. Behrens TEJ, Johansen-Berg H, Woolrich MW, et al. Non-invasive mapping of connections between human thalamus and cortex using diffusion imaging. *Nat Neurosci*. 2003;6:750-757.
46. Thalamic Connectivity Atlas n.d. https://fsl.fmrib.ox.ac.uk/connect/ (accessed September 5, 2019).
47. Jacobs HIL, Hedden T, Schultz AP, et al. Structural tract alterations predict downstream tau accumulation in amyloid-positive older individuals. *Nat Neurosci*. 2018;21:424-431.
48. Corder EH, Ghebremedhin E, Taylor MG, Thal DR, Ohm TG, Braak H. The biphasic relationship between regional brain senile plaque and neurofibrillary tangle distributions: modification by age, sex, and APOE polymorphism. *Ann N Y Acad Sci*. 2004;1019:24-28.

SUPPORTING INFORMATION

Additional supporting information may be found online in the Supporting Information section at the end of the article.

How to cite this article: Keator DB, Phelan MJ, Taylor L, et al. Down syndrome: Distribution of brain amyloid in mild cognitive impairment. *Alzheimer's Dement*. 2020;12:e12013. https://doi.org/10.1002/dad2.12013